Biochemical Engineering Journal 212 (2024) 109531

Contents lists available at ScienceDirect

Biochemical Engineering Journal

journal homepage: www.elsevier.com/locate/bej

Regular article

Removal of selenate from wastewater using a bioelectrochemical reactor: The importance of measuring selenide and the role of competing anions

Benhur K. Asefaw [a], Huan Chen [b,*], Youneng Tang [a,*]

[a] Department of Civil and Environmental Engineering, FAMU-FSU College of Engineering, Florida State University, 2525 Pottsdamer Street, Tallahassee, FL 32310, United States

[b] National High Magnetic Field Laboratory, Florida State University, 1800 East Paul Dirac Drive, Tallahassee, FL 32310, United States

ARTICLE INFO

Keywords:
Bioelectrochemical reactor
Nitrate
Selenide
Selenate
Sulfate

ABSTRACT

Removal of selenate (SeO_4^{2-}) from selenate-contaminated wastewater is challenging due to the commonly co-existing and competing anions of sulfate (SO_4^{2-}) and nitrate (NO_3^-). This study investigates SeO_4^{2-} reduction to elemental selenium (Se^0) in a cathode-based bioelectrochemical (BEC) reactor and a conventional biofilm reactor (*i.e.*, an upflow anaerobic reactor). The simulated wastewater contained SeO_4^{2-} at a typical concentration of 5 mg Se/L, SO_4^{2-} at a typical concentration of 1000 mg S/L, and NO_3^- at concentrations that varied from 0 to 10 mg N/L. The impact of sulfate on the BEC reactor was much lower than that on the conventional reactor: The selenium removal, defined as (selenate in influent – dissolved selenium in effluent)/selenate in influent, was 99 % in the BEC reactor versus 69 % in the conventional biofilm reactor. The lower selenium removal in the conventional reactor was mainly due to the >10 times higher reduction of sulfate, which directly caused competition between sulfate and selenate for the common resources such as electrons. The more reduction of sulfate in the conventional reactor further led to 45 times higher production of selenide. Selenide is usually assumed to be minimal and therefore not measured in the literature. This simplification may significantly overestimate selenium removal when the influent sulfate concentration is very high. NO_3^- in the influent of the BEC reactor promoted selenium removal when it was less than 5.0 mg N/L but inhibited selenate removal when it was more than 7.5 mg N/L. This was supported by the microbial community analysis and intermediate (nitrite) analysis.

1. Introduction

Selenium, a member of the chalcogen family, is a metalloid naturally occurring trace element on the Earth's crust [1]. Selenium exists in various oxidation states (+6, +4, 0, and −2) and can be found in both organic and inorganic forms. Selenium is essential for human health and can be obtained from dietary sources. As an antioxidant, it scavenges free radicals, supports the immune system, and is required to synthesize numerous proteins [2,3]. However, high concentrations of the soluble forms of selenium, selenate, and selenite (>50 μg Se/L) are toxic to humans and can bio-accumulate in the surrounding food chain [4]. The elemental selenium is the least toxic and insoluble in water [5–7]. The United States Environmental Protection Agency (USEPA) has established a maximum contaminant level of 50 μg Se/L in drinking water [8] and 76 μg Se/L as the maximum limit discharged from industries such as flue gas desulfurization (FGD) plants [9]. Selenium is mainly produced as a by-product during copper electrolytic refining in the anodic slimes [10]. It is extensively used in the glass and ceramic industry for coloring and has applications in the electronic industry due to its photovoltaic and photoconductive properties [11–13].

Selenium is also found in the wastewater of various industries, such as mining (1.6 mg/L – 7 mg/L) [14,15], FGD (1 μg/L – 10 mg/L) [1,15], petrochemical industry (7.5 μg/L – 4.9 mg/L) [14,15], coal fired power plants (0.4 μg/L – 1.5 mg/L) [1,14,15], and agricultural drainage (~1.4 mg/L) [15]. Selenium removal from wastewater can be achieved through various methods, including adsorption [16,17], photocatalysis [18,19], reverse osmosis [20–22], zero-valent iron [23,24], ion-exchange [21,25], chemical precipitation [26], and bioremediation [27–30]. While most of these chemical/physical methods are efficient, they are often expensive due to the high usage of chemicals or energy [31]. Bioremediation is a sustainable and inexpensive method for eliminating selenium contamination from wastewater by converting the soluble selenium oxyanions to insoluble elemental Se^0 through microbial catalysis.

* Corresponding authors.
E-mail addresses: huan.chen@magnet.fsu.edu (H. Chen), ytang@eng.famu.fsu.edu (Y. Tang).

https://doi.org/10.1016/j.bej.2024.109531
Received 1 August 2024; Received in revised form 24 September 2024; Accepted 11 October 2024
Available online 15 October 2024

SO_4^{2-} and NO_3^- are common co-existing dissolved anions in selenium-laden wastewater, particularly in agricultural drainages, FGD, and mining-impacted wastewater [27,32,33]. The concentrations of SO_4^{2-} and NO_3^- in FGD and mining-impacted wastewater vary from 525 to 6000 mg SO_4^{2-}/L and 1–400 mg NO_3^-/L, respectively [4,34]. Both anions are electron acceptors and can affect the removal efficiency of SeO_4^{2-}. SO_4^{2-}, which is abundant in water systems, may impact both the removal efficiency of SeO_4^{2-} and the recovery of pure Se^0 due to the possible formation of selenium sulfides [35,36]. Various microbial species can simultaneously reduce SeO_4^{2-} and SO_4^{2-}, making SO_4^{2-} a competitor for SeO_4^{2-} reduction [37,38]. Previous reports have explored the effects of SO_4^{2-} on SeO_4^{2-} reduction in some bioreactors. For instance, a biofilm composed of mostly a SO_4^{2-} reducing species, *Desulfomicrobium norvegicums*, was reported to reduce more SeO_4^{2-} in the presence of excess SO_4^{2-} (2800 mg/L) [38]. Zhang et al. demonstrated higher removal of SeO_4^{2-} in a membrane biofilm reactor (MBfR) in the presence of SO_4^{2-} (4500 mg/L) at the optimum flow rate [36]. Conversely, Tan et al. reported lower SeO_4^{2-} reduction efficiency under elevated SO_4^{2-} concentration (1500 mg/L) in an up-flow anaerobic sludge blanket (UASB) reactor [39]. Selenium and sulfur, both in the same group on the periodic table, have analogous reactions due to their similar chemical properties [40]. In reactors with excess SO_4^{2-}, biological reduction of the intermediate product selenite (SeO_3^{2-}) can form selenium sulfides, affecting the purity of Se^0 nanoparticles during recovery [41]. Previous studies have advanced the understanding of the interactions between SO_4^{2-} and SeO_4^{2-} in the microbial removal of SeO_4^{2-} using conventional biological reactors such as MBfR and UASB [37,38].

A bioelectrochemical (BEC) reactor utilizes microbial metabolism to produce electrons on the biotic anode and transport them from the anode chamber to the abiotic cathodes, effectively reducing metals such as Co^{2+}, Cd^{2+}, Hg^{2+}, Au^{3+}, Cr^{6+}, Se^{6+}, Ni^{2+}, Ag^+, and Cu^{2+} [42–44]. Biocathodes of BEC reactors have been much less studied than abiotic cathodes. Biocathodes have shown efficiency in removing SeO_4^{2-} and producing extracellular elemental Se^0 for easy recovery [29,31]. Nevertheless, the effects of SO_4^{2-} concentrations on the reduction of SeO_4^{2-} to elemental Se^0 in the BEC reactor have not been reported. The primary objective of this study is to investigate the effects of high loading rate of SO_4^{2-} on SeO_4^{2-} reduction using BEC reactors and determine the optimal operating conditions for efficient recovery of elemental Se^0 from wastewater.

Similar to SO_4^{2-}, NO_3^- is another electron acceptor that may inhibit the reduction of SeO_4^{2-} if its concentration is high [32,45]. The literature on the effects of NO_3^- on SeO_4^{2-} reduction is inconsistent. Some studies indicate that NO_3^- inhibits SeO_4^{2-} reduction due to its thermodynamic preference of NO_3^- over SeO_4^{2-} and competition for shared resources such as electron donors, reductases, or components in the reduction pathway [46,47]. Other studies suggest that NO_3^- has no effect on SeO_4^{2-} reduction [48–50], while others demonstrate that NO_3^- promotes the reduction of SeO_4^{2-} since NO_3^- induces a reductase for SeO_4^{2-} reduction or serves as the primary electron acceptor [51,52]. The inconsistency in the reported interaction between NO_3^- and SeO_4^{2-} in bioreactors suggests that the effect may depend on the NO_3^- to SeO_4^{2-} loading rate since the loadings (*i.e.* concentrations and flow rates) affect the thermodynamics and their degree of inhibition or promotion. This study is the first to examine the interactions of NO_3^-, SO_4^{2-}, and SeO_4^{2-} on the biocathode of the BEC reactor, which constitutes the second objective of this paper. Additionally, this research investigates the changes in the microbial communities help further understand the mechanisms underlying the interactions of NO_3^-, SO_4^{2-}, and SeO_4^{2-}.

2. Materials and methods

2.1. Experimental setup

A BEC reactor (Figure S1) and a conventional biofilm reactor (Figure S2) were set up in an anaerobic environment. The BEC reactor was constructed with H-shaped glass bottles (Adams & Chittenden Scientific Glass, USA) separated by a cation exchange membrane (CEM, model CMI-7000, Membrane International Inc., USA). Each chamber had a working liquid volume of 270 mL, with 80 mL pure nitrogen gas at the head space. Graphite carbon cloth electrodes (3 cm × 5 cm, Fuel cell Store, USA) were used in the anode and cathode chambers, remaining completely submerged during the experimental period. The carbon clothes were inoculated with an anaerobic mixed culture enriched from a local municipal wastewater treatment plant for 15 days before being used in the BEC reactor. The electrodes were connected to a 100 Ω external resistor with a copper wire throughout the experiment (Stages 1–10). Pieces of membrane (0.1 μm pore diameter, Nuclepore track-etched membranes, Whatman, USA) were put at the bottom of the chambers to collect precipitates for analysis. The conventional reactor, used as a control, consisted of a column filled with plastic media (Bio-FLO 9, Smoky Mountain Bio Media) designed for biofilm attachment (details about the reactor and the operating conditions used are provided in Table S1). The experiment was conducted at 30 ^{0}C.

2.2. Operation of the reactors

After inoculating the carbon cloth electrodes of the BEC reactor and the plastic media of the conventional reactor with the mixed culture, the carbon cloth electrodes were transferred to the anode and cathode chambers of the BEC reactor, and the plastic media to the conventional reactor. A synthetic media [31] amended with sodium acetate (CH_3COONa, 10 mg C/L) as a sole electron donor was fed to the anode chamber. The cathode chamber was fed with similar media but with the addition of sodium selenate (Na_2SeO_4, 5 mg Se/L), sodium sulfate (Na_2SO_4, 5 mg S/L, 1000 mg S/L), and sodium nitrate ($NaNO_3$, 2.5 mg N/L, 5 mg N/L, 7.5 mg N/L, and 10 mg N/L) as electron acceptors at different stages of the experiment. This synthetic media is used to simulate the industrial wastewater in our study.

The continuous-based BEC reactor was conducted in multiple stages, as indicated in Table 1, to determine the ideal operating conditions for the maximum reduction of SeO_4^{2-} to elemental Se^0 from selenium-containing FGD wastewater. The pH of the influent anaerobic medium was maintained at 7.0. The concentration ratio of acetate to selenate was kept greater than 2:1 to ensure that acetate was not a limiting factor. The hydraulic retention time (HRT) in the cathode chamber of BEC reactor varied from 0.75 days to 1.5 days, corresponding to a SeO_4^{2-} loading rate of 660 − 330 mg Se/m^2-day, respectively (Table 1). The SeO_4^{2-} loading rate in the conventional reactor was kept the same as the BEC reactor at the corresponding stages of operation.

2.3. Sampling and Chemical Analysis

Influent and effluent samples from both chambers of the BEC and conventional reactors were collected approximately once a week. Dissolved selenium species (SeO_4^{2-}, SeO_3^{2-}, selenide (Se^{2-})), solid Se in the effluent, solid Se in the reactor, and other dissolved chemical species such as acetate, NO_3^-, nitrite (NO_2^-), SO_4^{2-}, sulfite (SO_3^{2-}), and sulfide (S^{2-}) were measured. The influent and effluent dissolved SeO_4^{2-}, SeO_3^{2-}, NO_3^-, NO_2^-, SO_4^{2-}, and SO_3^{2-} were measured using Ion chromatography (IC, Dionex Aquion Ion Chromatography System, USA). S^{2-} was measured using a UV-Vis spectrophotometer (UV-2501 PC, Shimadzu, USA), with the absorbance recorded at 664 ± 10 nm [53]. The quantification of selenide (Se^{2-}) was performed using two methods for cross-checking. The direct measurement method was performed in triplicate based on the reaction between Se^{2-} and 2,3-diaminonaphthalene (DAN) to form a red-colored complex [54,55]. The absorbance of the complex mixture was measured at a wavelength around 520–530 nm using a UV-Vis spectrophotometer (Agilent 8453 UV-Vis, USA). The indirect calculation method was based on mass balance and involved the difference between the total soluble selenium in the effluent sample (after filtration through a 20 nm-pore size syringe and centrifuged at 21,000 × g for

Table 1
Operating conditions of each stage in the bioelectrochemical reactor.

Stages	HRT (days)		Loading rate (mg Se/m^2-day)		Acetate (mg C/L)	SeO_4^{2-} (mg Se/L)	NO_3^- (mg N/L)	SO_4^{2-} (mg S/L)	
	Cathode	Anode	Cathode	Anode	Anode	Cathode	Cathode	Cathode	Anode
1	1.45	1.45	330	660	10	5	-	5	5
2	1.45	1.45	330	660	10	5	-	1000	1000
3	0.75	1.45	660	660	10	5	-	1000	1000
4	0.75	1.45	660	660	10	5	-	1000	5
5	0.75	1.45	660	660	10	5	-	5	5
6	1.45	1.45	330	660	10	5	-	1000	5
7	1.45	1.45	330	660	10	5	2.5	1000	5
8	1.45	1.45	330	660	10	5	5	1000	5
9	1.45	1.45	330	660	10	5	7.5	1000	5
10	1.45	1.45	330	660	10	5	10	1000	5

30 min) and the dissolved effluent selenium ($[SeO_4^{2-}]_{eff} + [SeO_3^{2-}]_{eff}$). To measure the total selenium and total dissolved selenium (after sample filtration and centrifugation) at the effluent, a microwave plasma - atomic emission spectrometer (4100 MP-AES, Agilent Technologies, USA) was used. The solid Se in the effluent was computed from the mass balance by taking the difference between total soluble selenium in the effluent sample and total soluble selenium in the effluent sample (after filtration through a 20 nm-pore size syringe and centrifugation at 21, 000 × g for 30 min). The difference between total soluble solid selenium and effluent solid selenium is the total solid selenium precipitated in the reactor. Methane produced in each chamber's headspace was measured using Gas chromatography (GC, model SRI 8610 C, SRI instruments, USA). Throughout the experiment, the pH of the effluent samples was 7.1 ± 0.2.

Coulombic efficiency was used to assess the electrochemical performance of the BEC reactor. It was calculated by dividing the number of electrons transferred from the anode to the cathode electrode by the concentration of acetate (electron donor) consumed in the anode chamber. Details are provided in the supplementary information (SI).

Solid samples were collected at the end of each stage from different locations of the BEC reactor for further characterization. The locations include the anode electrode, cathode electrode, precipitate collected at the bottom of the cathode chamber, and the retentate collected after filtering the cathode effluent samples using a 100 nm membrane filter. These samples were pretreated according to Zhang et al. [29] and analyzed using Scanning Electron Microscopy (SEM, FEI Nova 400 Nano SEM, FEI, USA) coupled with Energy Dispersive X-ray (EDX).

2.4. Microbial community analysis

We analyzed the microbial community by collecting biomass samples from various locations of the BEC reactor during various stages. Specifically, we obtained samples from the anode chamber during stages 1–5 and from the cathode chamber during stages 1–10. In the anode chamber, no changes were made to the operating conditions after stage 5 (*e.g.*, flow rate and acetate concentration), so we did not perform additional microbial community analysis. An inoculum sample was also collected at the beginning of the experiment. Illumina MiSeq sequencer (MiSeq, Illumina, USA) was used to analyze the 16S rRNA gene-targeted amplicon sequencing and followed a two-step PCR amplification protocol modified from Pylro et al. [56] and Ionescu et al. [57]. Details on the sequencing and analysis are provided in the supporting information. R with package Superheat was used to generate heat maps [58]. DNA extraction protocol was based on our previous study [29].

3. Results and discussions

3.1. SeO_4^{2-} reduction in the BEC reactor

Stages 1 and 2 were used to evaluate the effects of the SO_4^{2-} concentration. At the steady state of stage 1, with a low concentration (5 mg S/L) of SO_4^{2-} in anode and cathode chambers, 4.8 mg Se/L of SeO_4^{2-} was converted to solid Se^0 and 0.11 mg Se/L of Se^{2-} was produced (Fig. 1A). In the cathode effluent, SeO_4^{2-} and SeO_3^{2-} were below the quantification limits. The increase in influent SO_4^{2-} concentration (1000 mg S/L, a typical concentration in SeO_4^{2-}-laden wastewater) in both chambers during stage 2 negatively impacted the reactor's Coulombic efficiency due to competition for electrons at the anode chamber. This further affected SeO_4^{2-} reduction efficiency in the cathode chamber. At the steady state of stage 2, the total solid Se^0 produced decreased to 4 mg Se/L. The total effluent concentrations of total dissolved selenium (SeO_4^{2-}, SeO_3^{2-}, and Se^{2-}) increased to 1.31 mg Se/L. In summary, the high SO_4^{2-} concentration resulted in incomplete removal of SeO_4^{2-}, more accumulation of the intermediate SeO_3^{2-} and less production of Se^0 and Se^{2-}.

Stages 3–5 were used to evaluate the effects of flow rate in the cathodic chamber: 400 mL/day in stages 3–5 compared to 200 mL/day in stages 1 and 2. In stage 3, the high cathodic flow rate caused accumulation of more SeO_3^{2-} (~1.2 mg Se/L) in the cathode effluent. Only 3.33 mg Se/L of elemental Se^0 was produced at the steady state of stage 3. The effluent concentrations of SeO_4^{2-} and Se^{2-} were 0.45 mg Se/L and 0.02 mg Se/L, respectively. Under stage 4, the influent SO_4^{2-} concentration at the anode chamber was reduced from 1000 to 5 mg S/L. We continuously monitored the ionic strength of the anode media and maintained it at a constant level by adding biocabonates (1.2 g/L). The Coulombic efficiency increased, leading to a substantial flow of electrons across an external resistor to the biocathode (Figure S3). Despite the high influent flow rate (400 mL/day) corresponding to higher loading rates of SeO_4^{2-} and SO_4^{2-} at the cathode chamber in stage 4, the substantial flow of electrons to the cathode electrode promoted further reduction of SeO_4^{2-} and SeO_3^{2-} to elemental Se^0. Under the steady state of stage 4, the total elemental Se^0 produced increased to 3.84 mg Se/L (a 15 % increase when compared with the preceding stage) with 0.96 mg Se/L SeO_3^{2-}, 0.16 mg Se/L SeO_4^{2-}, and 0.04 mg Se/L Se^{2-} in the cathode effluent. In stage 5, the SO_4^{2-} concentration in the cathode chamber was reduced from 1000 to 5 mg S/L. During the steady state of stage 5, the total elemental Se^0 produced further increased by ~31 % to 4.37 mg Se/L compared to stage 3. The total dissolved selenium in the effluent was 0.63 mg Se/L (Table 2). In summary, the higher flow rate in the cathode chamber for stage 5 resulted in higher total dissolved selenium in the effluent (*i.e.*, 0.63 mg Se/L) than stage 1 (*i.e.*, 0.11 mg Se/L) while all the other operating conditions were the same. The total dissolved selenium was above the USEPA standard for industrial wastewater of 0.076 mg/L in all the five stages.

Stages 6–10 were used to evaluate the combined effects of SO_4^{2-} (1000 mg/L) and NO_3^- (0 mg/L in stage 6, 2.5 mg N/L in stage 7, 5.0 mg N/L in stage 8, 7.5 mg N/L in stage 9, and 10.0 mg N/L in stage 10) on SeO_4^{2-} (5.0 mg Se/L) removal at a flow rate of 200 mL/day for the cathode chamber, which was the same as in stage 1. At steady state, the total dissolved selenium in the effluent reached the minimum of 0.050 mg Se/L in stage 8, corresponding to an influent NO_3^- concentration of 5.0 mg N/L. This was the only stage that met the USEPA standard

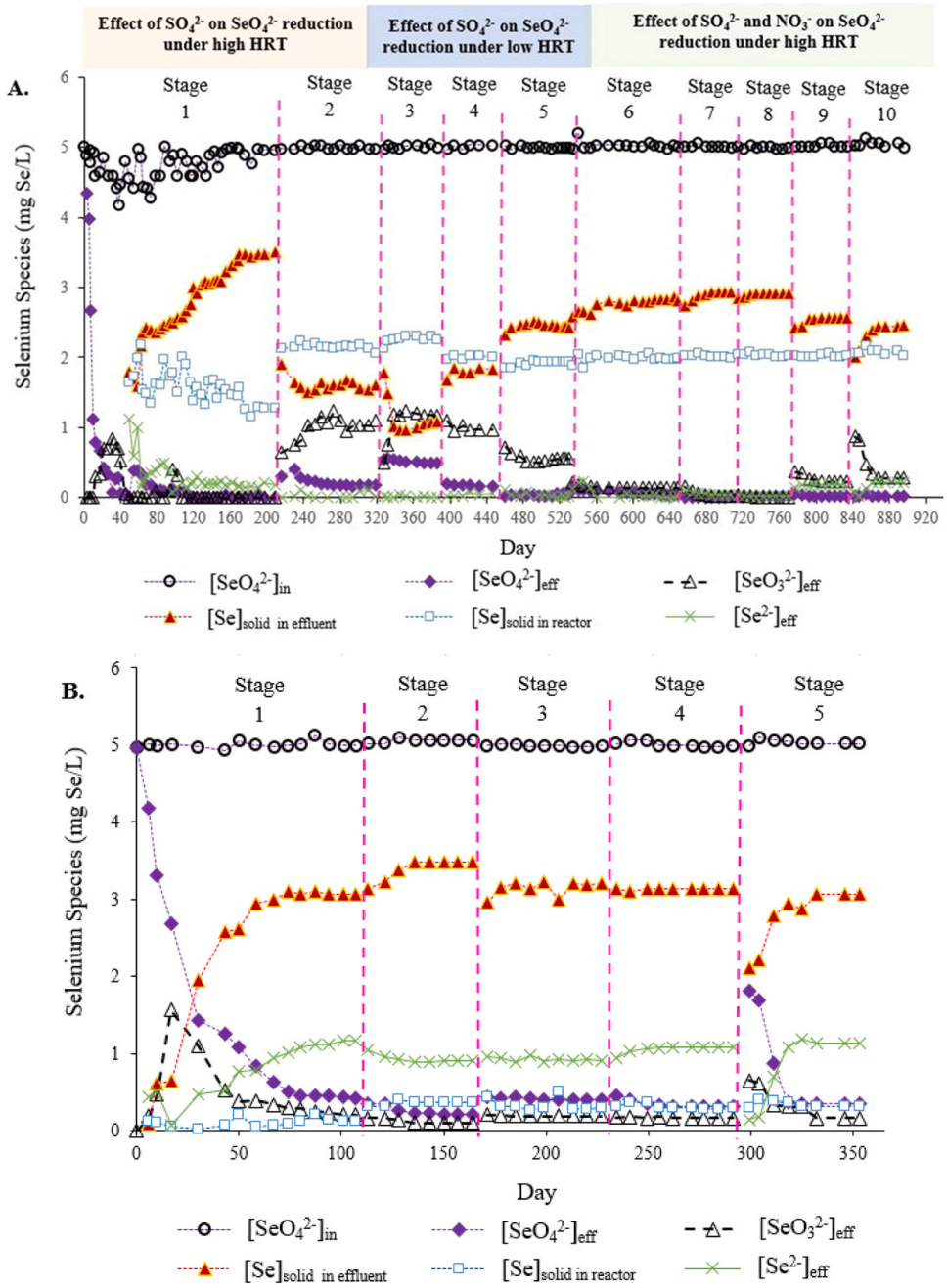

Fig. 1. Selenate reduction in the cathodic chamber of BEC reactor (A) and the conventional reactor (B). Note: Stages 1–5 in the conventional reactor correspond to Stages 6–10 in the BEC reactor. Note: High HRT ≥1.25 days, Low HRT ≤0.75 days.

of 0.076 mg Se/L. When the NO_3^- concentration was 5.0 mg N/L or less in stages 6–8, more nitrate promoted selenate reduction by decreasing the total dissolved selenium in the effluent: 0.20 mg Se/L for stage 6, 0.08 mg Se/L in stage 7, and 0.05 mg Se/L in stage 8. NO_3^- is known in the literature to induce selenate reductase [27,52,59]. When NO_3^- concentration was 7.5 mg N/L or more in stages 9–10, more nitrate inhibited selenate reduction by increasing the total dissolved selenium in the effluent: 0.42 mg Se/L for stage 9 and 0.52 mg Se/L for stage 10. The inhibition was due to competition for limited common resources such as electrons. Evidence for limited electrons was low nitrate reduction (2.2–3.2 mg N/L in effluent; See Table 2) and significant accumulation of intermediate (*i.e.*, nitrite = 0.6–0.8 mg N/L in Table 2) only in stages 9 and 10.

3.2. SeO_4^{2-} reduction in the conventional biofilm reactor

The conventional biofilm reactor was operated for five stages to mimic and compare to stages 6–10, respectively, in the BEC reactor. During the five stages, the nitrate concentration in the influent varied from 0 to 10.0 mg N/L while sulfate was fixed at 1000 mg S/L and selenate was fixed at 5 mg Se/L. Surprisingly, the lowest total dissolved selenium species at the effluent was 1.22 mg Se/L (Fig. 1B and Table 3), 16 times higher than the limit of 0.076 mg Se/L set by USEPA for FGD wastewater. The selenium removal efficiency, calculated as (selenate in the influent – dissolved selenium in the effluent)/selenate in the influent, was 69.2 % (Table 3). This removal was close to the lower end of the range reported in the literature (60–100 %). The direct reason was the production of high concentration of selenide during all of the five stages (Fig. 1B). Selenide was measured and reported in only one of the

Table 2
Bioelectrochemical reactor performance at steady state of various stages.

		Experimental Stages→	1	2	3	4	5	6	7	8	9	10
Cathode Chamber	Operating condition	Flow rate (mL/day)	200	200	400	400	400	200	200	200	200	200
		SeO_4^{2-} surface loading rate (mg Se/m^2-day)	330	330	660	660	660	330	330	330	330	330
	Reactor performance	SeO_4^{2-} in influent (mg Se/L)	~4.90	~4.97	~5.0	~5.0	~5.0	~5.0	~5.0	~5.0	~5.0	~5.0
		SeO_4^{2-} in effluent (mg Se/L)	BQL[1]	~0.18	~0.45	~0.16	~0.05	~0.04	BQL	BQL	BQL	BQL
		SeO_3^{2-} in effluent (mg Se/L)	BQL	~1.1	~1.2	~0.96	~0.56	~0.14	~0.03	BQL	~0.23	~0.28
		Se^{2-} in effluent (mg Se/L)	~0.11	~0.03	BQL	~0.04	BQL	BQL	~0.03	BQL	~0.17	~0.22
		Particulate Se (mg Se/L)	~4.80	~3.66	~3.33	~3.84	~4.37	~4.9	~4.92	~4.95	~4.58	~4.48
		SeO_4^{2-} removal efficiency (%)	~99.8 %	~73.6 %	~66.6 %	~85.6 %	~87.4 %	~97.6 %	~98.4 %	~99 %	~91.6 %	~89.6 %
		SO_4^{2-} in influent (mg S/L)	~5.0	~1000.0	~1000.0	~1000.0	~5.0	~1000.0	~1000.0	~1000.0	~1000.0	~1000.0
		SO_4^{2-} in effluent (mg S/L)	~4.9	~997.8	~998.7	~998.7	~4.9	~997.6	~996.6	~993.4	~994.4	~994.5
		SO_3^{2-} in effluent (mg S/L)	BQL	BQL	BQL	BQL	BQL	BQL	BQL	BQL	BQL	BQL
		S^{2-} in effluent (mg S/L)	BQL	BQL	BQL	BQL	BQL	BQL	BQL	BQL	BQL	BQL
		NO_3 in influent (mg N/L)	-	-	-	-	-	-	~2.5	~5.0	~7.5	~10.0
		NO_3 in effluent (mg N/L)	-	-	-	-	-	-	~0.07	~0.08	~2.2	~3.2
		NO_2 in effluent (mg N/L)	-	-	-	-	-	-	~0.06	~0.01	~0.61	~0.8
	Operating condition	Flow rate (mL/day)	200	200	200	200	200	200	200	200	200	200
Anode Chamber		Acetate surface loading rate (mg C/m^2-day)	660	660	660	660	660	660	660	660	660	660
	Reactor performance	Acetate in influent (mg C/L)	~10.0	~10.0	~10.0	~10.0	~10.0	~10.0	~10.0	~10.0	~10.0	~10.0
		Acetate in effluent (mg C/L)	~1.3	~0.3	~0.3	~1.26	~1.28	~1.29	~1.27	~1.27	~1.28	~1.27
		SO_4^{2-} in influent (mg S/L)	~5.0	~1000.0	~1000.0	~5.0	~5.0	~5.0	~5.0	~5.0	~5.0	~5.0
		SO_4^{2-} in effluent (mg S/L)	~4.2	~993.0	~993.0	~4.3	~4.3	~4.47	~4.46	~4.48	~4.47	~4.47
		SO_3^{2-} in effluent (mg S/L)	BQL	BQL	BQL	BQL	BQL	BQL	BQL	BQL	BQL	BQL
		S^{2-} in effluent (mg S/L)	BQL	BQL	BQL	BQL	BQL	BQL	BQL	BQL	BQL	BQL

Notes: [1]BQL = below quantification limit (< 0.02 mg/L); SeO_4^{2-} removal efficiency(%) = (1- (effluent SeO_4^{2-}+ SeO_3^{2-})/ influent SeO_4^{2-})× 100, Particulate Se recovery efficiency(%) = (Particulate Se/ influent SeO_4^{2-}) × 100

fifteen previous studies (Table 3). It is common in the literature to neglect selenide production. However, our study shows that this common practice may significantly overestimate the selenium removal efficiency. The measurement of selenide is particularly important when treating wastewater containing selenate and a high concentration of sulfate since the sulfate reduction intermediate (*i.e.*, sulfite) can participate in the production of selenide [60,61].

The lower selenium removal efficiency in the conventional reactor (69.2 %) compared to the BEC reactor (99.0 %) in our study could possibly be explained by the following two reasons. First, the sulfate reduction efficiency was more than 10 times higher in the conventional reactor (4.9 % in Table 3) compared to the BEC reactor (0.3 % in Table 3). This means more competition between sulfate and selenate reduction in the conventional reactor than in the BEC reactor, which is further explained by the microbial community analysis in the microbial community analysis section: The cathode chamber of the BEC reactor showed high activity and dominancy of electroactive selenate-reducing bacteria compared to the other species. The second reason was associated with the first reason. More sulfate reduction leads to the production of more intermediate (*i.e.*, sulfite), which could promote selenide production in the conventional reactor.

Fig. 2 shows consistent results between the two methods for quantification of selenide: the direct measurement method and the indirect calculation method. The corresponding samples were collected at the steady state of stages 6–10 for the BEC reactor and stages 1–5 for the conventional reactor. During these stages, the reactor operation was comparable between the two reactors and the sulfate concentration was high (1000 mg S/L). Notably, in stage 8, the BEC reactor had a minimal selenide concentration of 20 μg Se/L, while the conventional reactor exhibited a significantly higher concentration of 980 μg Se/L (Fig. 2). The discussion on selenide adds a unique and rigorous dimension to this study, underscoring the difference of the two reactors operated under high sulfate concentration.

3.3. Characterization of particles in the bioelectrochemical reactor

The SEM images in Fig. 3, S5, and S6 revealed the accumulation of dense and spherical nanoparticles around the rod-shaped microorganisms at various stages of the experiment. Further analysis using the EDX spectra unequivocally verified that the dense, spherical nanoparticles accumulated on the biocathode, cathode effluent, and precipitates collected from the bottom of the cathode chamber were elemental selenium nanoparticles. Contrasting peak sizes between Se and the other elements (C, O, S, and P) indicated that elemental Se^0 was retained as the highest element within the particulate samples from the cathode chamber. At stage 1, Fig. 4 shows that selenium was 33 % in the precipitates at the bottom of the cathode chamber, 36 % in the cathode effluent, and 55 % in the cathode biofilm matrix. These numbers suggest high potential for selenium recovery.

To show the effects of high sulfate concentration on the potential recovery of selenium, Fig. 4 compares the elemental compositions of particulate samples in the cathode chamber between stage 1 (5 mg SO_4^{2-}-S/L in the influent) and stage 4 (1000 mg SO_4^{2-}-S/L in the influent). The higher sulfate concentration in stage 4 resulted in lower selenium weigh percentage (27 % - 37 %) than stage 1 (33 % - 55 %). Selenium was still the most abundant in the particulate samples from the cathode in stage 4, when the sulfate concentration was 200 times higher in the influent than in stage 1.

3.4. Microbial community analysis

Microbial community analysis of the inoculum and the biomass collected from different locations of the BEC reactor at each stage of the experiment was performed. Biomass samples included both suspended biomass and biofilms attached to electrodes collected at steady states. The heatmaps in Figs. 5 and 6 display the OTUs across 31 samples,

Table 3
Comparison of bioreactors on selenate removal.

Reactor	HRT (hrs)	Electron donor loading rate	SeO_4^{2-} in influent (mg Se/L)	SeO_4^{2-} and SeO_3^{2-} in effluent (mg Se/L)	Se^{2-} in effluent (mg Se/L)	Se removal (%)	NO_3^- in influent (mg N/L)	NO_3^- removal (%)	SO_4^{2-} in influent (mg S/L)	SO_4^{2-} removal (%)	References
BEC[b]	35.0	Acetate (10 mg C/L)	5.0	0.03	0.02	99.0 %	5.0	98.6 %	999.8[a]	0.3 %	This study (stage 8)
Conventional reactor (upflow anerobic reactor)[b]	0.73	Acetate (10 mg C/L)	5.0	0.63	0.91	69.2 %	5.0	99.4 %	999.9	4.9 %	This study (stage 2)
Conventional reactor (MBfR)	6.72	127 mg H_2/m^2.day	4.0	0.05	0.02	98.3 %	-	-	1526	0.2 %	[4]
Conventional reactor (MBfR)	3.3	180 mg H_2/m^2.day	1.4	0.04	NM	97.0 %	-	-	90	25.0 %	[78]
Conventional reactor (MBfR)	20.0	H_2, 5.8 psi	2.0	0.02	NM	99.0 %	10.0	99.8 %	50	26.0 %	[79]
Conventional reactor (MBfR)	0.4	H_2, 2.5 psi	1.0	0.19	-	81.0 %	4.0	99.8 %	40	7.5 %	[80]
Conventional reactor (MBfR)	2.17	H_2, 15 psi	1.00	0.4	-	60.0 %	10.0	70.0 %	-	-	[27]
Conventional reactor (Drip flow reactor)	41.0	Lactate (666 mg C/L)	10.0	2.1	NM	77.0 %	67.2	95.0 %	416	5.0 %	[32]
Conventional reactor (Biotrickling filter)	11.3	Lactate (666 mg C/L)	12	1.2	NM	90.0 %	-		400	75.0 %	[81]
Conventional reactor (Sludge blanket reactor)	2.33	Acetate (72 mg C/L)	0.55	0.001	NM	98.2 %	64.6	97.8 %	1550	27.0 %	[82]
Conventional reactor (Fluidized bed reactor)	12	Ethanol (240 mg C/L)	395	0.01	NM	100.0 %	70.0	100.0 %	-	-	[83]
Conventional reactor (Inverse fluidized bed reactor)	12	Ethanol (240 mg C/L)	395	0.79	NM	99.8 %	70.0	100.0 %	670	1.5 %	[33]
Conventional reactor (Attached growth bioreactor)	1.0	Acetate (48 mg C/L)	0.3	0.01	NM	96.0 %	11.3	99.8 %	16.6	97.0 %	[84]
Conventional reactor (UASB)	24.0	Lactate (830 mg C/L)	7.9	1.58	NM	80.0 %	56.0	80.0 %	1440	30.0 %	[85]
Conventional reactor (UASB)	24.0	Lactate (830 mg C/L)	12	4.5	NM	61.0 %	47.0	92.0 %	1500	15.0 %	[86]
Conventional reactor (UASB)	6.0	Lactate (720 mg C/L)	0.79	0.04	NM	95.0 %	210.0	90.0 %	64	10.0 %	[87]
Conventional reactor (UASB)	6.0[c]	Lactate (468 mg C/L)	0.79	0.008	NM	99.0 %	-	-	832	20.0 %	[88]

Notes: [a] At the cathode; Percentage removal = (Influent concentration - Effluent concentration)/Influent concentration;
[b] Selenate loading rate in BEC and Conventional reactor is 330 mg Se/m^2-day; [c] Liquid upflow 1 m/hr
MBfR: Membrane biofilm reactor; UASB: Upflow anaerobic Sludge blanket reactor; NM: not measured/shown

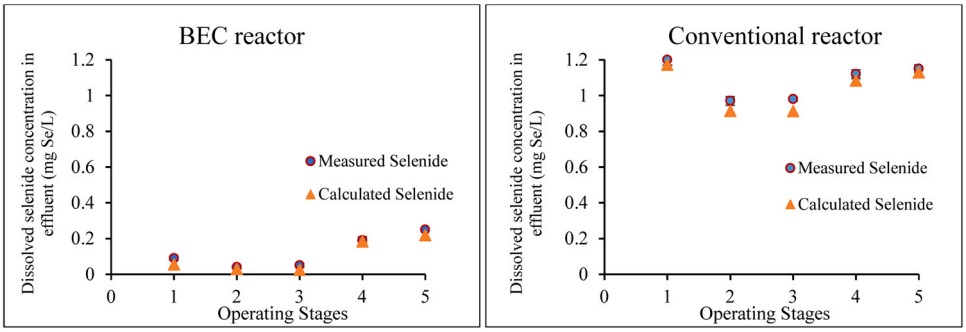

Fig. 2. Comparison of the direct measurement method and indirect calculation method for quantifying dissolved selenide (Se^{2-}) present in the effluent of BEC and conventional reactors at five steady states. Note: Stages 1–5in this figure corresponds to stages 6–10 in the text, respectively, for the BEC reactor.

including the inoculum, biocathode, cathodic effluent, bioanode, and anodic effluent, all taken at steady state for the BEC reactor. These heatmaps illustrate the relative abundance of the dominant genera within the anode and cathode chambers, respectively.

Geobacter, a well-known electroactive bacterium, was found to be enriched on the original inoculated carbon cloth and the anode of the BEC reactor across all stages (14–23 %). *Geobacter* directly transport electrons from its inner membrane to the anode using its pili [62,63].

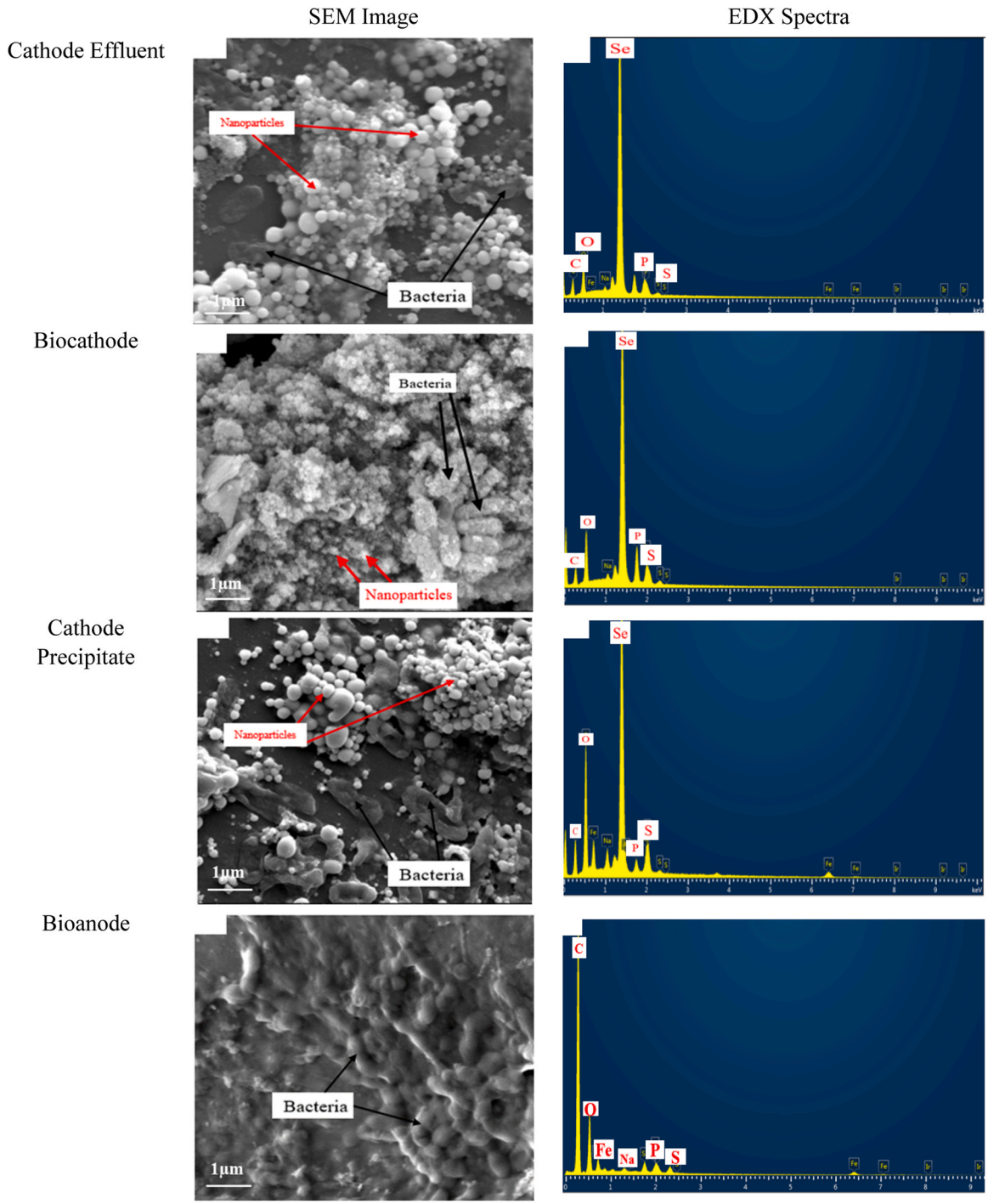

Fig. 3. Representative SEM images and EDX spectra for stage 6 of the BEC reactor. (Note: For each sample 50 SEM-EDX spectra were performed).

The second dominant electroactive genus on the anode across all stages was *Pseudomonas* (10–19.6 %), also well-known for its electron transfer ability on the anode [64,65]. The abundance of these two dominant genera was always much higher on the anode than in the anode chamber effluent. *Dechloromonas* was found in the inoculum at 5 % and ascended to the dominant genus on the anode in stage 1. *Dechloromonas* is an electroactive genus that can transfer electrons to the electrode extracellularly [66]. When sulfate increased from 5 mg S/L in stage 1–1000 mg S/L in stage 2, *Dechloromonas* was replaced by two genera well-known for sulfur-cycling ability and electron transfer ability: *Desulfovibrio* and *Thiobacillus* [67–69].

The microbial community in the cathode chamber from stages 1–10 was dominated by selenium-respiring bacteria of the genera *Delfia* (8–23 %), *Comamonas* (9–23 %), *Pseudomonas* (4–21 %), *Stenotrophomonas* (6–20 %), *Azospira* (3–16 %), as well as a sulfate respiring genus, *Desulfovibrio* (3–15 %) and a nitrate respiring genus, *Halomonas* (2–29 %). All these groups were gram-negative, curved to straight rod-shaped bacteria. Ghosh et al. first reported the association of the genus *Delftia* in SeO_4^{2-} reduction [70]. Zheng et al. identified that *Comamonas testosteroni* could reduce both SeO_4^{2-} and SeO_3^{2-} to elemental Se nanoparticles ranging in size from 0.1 to 0.2 µm outside the cells [71]. Previous studies reported the electro-activity of *Pseudomonas* by transferring electrons through a mediated process [64] and its ability to reduce SeO_4^{2-} and SeO_3^{2-} to elemental Se^0 nanoparticles both inside and

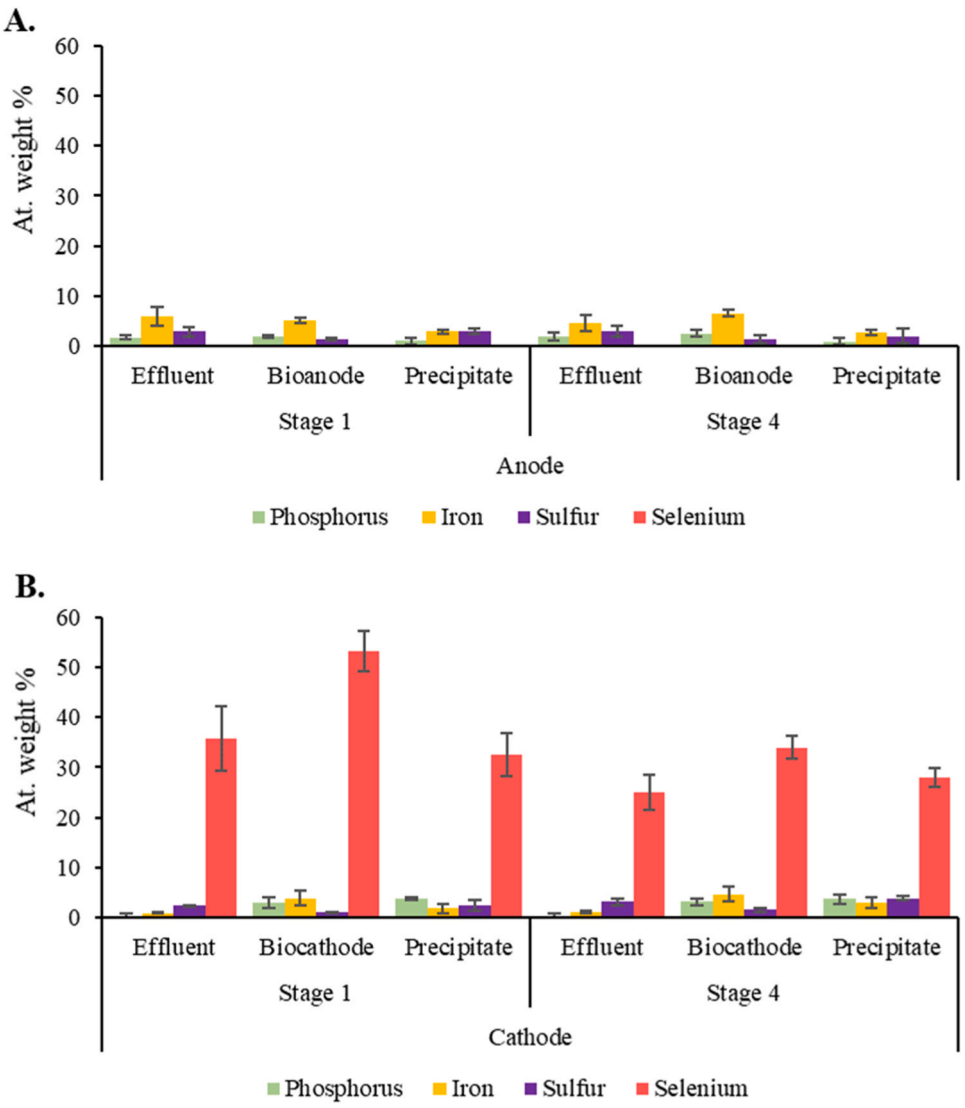

Fig. 4. Comparison of the atomic weight percentage (mean ± standard deviation) based on SEM-EDX mapping between stage 1 and stage 4 in the BEC reactor. Note: 50 EDX spectra were collected and evaluated for each sample.

outside the cells [32,72]. *Stenotrophomonas* was found on the biocathode of a BEC reactor, reducing SeO_4^{2-} to elemental Se^0 [29]. In MFCs, *Stenotrophomonas* extracellularly breakdown hydrocarbons derived from diesel [29,73]. The genus *Azospira* is known for its extracellular electron transfer ability using its c-type cytochrome in MFCs [29,74]. Despite the average low abundance of this genus on the biocathode, except in stage 1, it potentially aided the reduction of SeO_4^{2-} to elemental Se^0.

Accumulation of the genus *Desulfovibrio* in the cathode chamber was evident since the cathode chamber was loaded with a higher concentration of SO_4^{2-} in stage 2. Previous studies reported that *Desulfovibrio* species can form electroactive biofilms and grow well in the presence of both SO_4^{2-} and SeO_4^{2-} [32,75]. When NO_3^- was added to the cathode chamber in the last stages of the experiment (*i.e.*, stages 7–10), a larger percentage of the genus *Halomonas* was observed. *Halomonas sp.* is reported as an efficient nitrate reducer in high-salinity nitrogenous wastewater [76,77]. The microbial community analysis suggests that the BEC reactor's microbial community was dynamic and adapted to the changing conditions across different experimental stages. The enrichment of electroactive and selenium-respiring bacteria such as *Comamonas*, *Stenotrophomonas*, *Pseudomonas*, and *Delftia* underlines their significant role in facilitating the reduction processes. The presence of sulfate and nitrate reducers, such as *Desulfovibrio* and *Halomonas*, indicates the complex interplay of microbial species involved in electron transfer and reduction mechanisms. This comprehensive understanding of microbial community dynamics provides valuable insights into optimizing BEC reactors for efficient selenium removal from wastewater.

Figure S7 highlights the dominant genera on the biomass carrier in the conventional reactor, including *Halomonas* (3–18 %), *Pseudomonas* (12–15 %), *Azospira* (6–9 %), *Desulfovibrio* (11–14 %), *Desulfocapsa* (8–13 %), *Desulfotalea* (7–11 %), and *Stenotrophomonas* (11–13 %). Notably, *Halomonas, Pseudomonas*, *Azospira*, and *Stenotrophomonas* were among the dominant genera in the biocathode. The presence of *Desulfovibrio*, *Desulfocapsa*, *Desulfotalea* in the conventional reactor indicates a higher level of sulfate reduction, as these genera are well known for their sulfate-reducing capabilities [32,33,75]. This analysis helps explain why sulfate reduction was more pronounced in the conventional bioreactor than in the BEC system. In the BEC, selenate reduction was more selective over sulfate reduction, as suggested by the lower amount of sulfate reduction in the BEC compared to the conventional reactor. The dominance of sulfate-reducing bacteria in the conventional reactor further supports this observation.

Fig. 7 shows the weighted PCA analysis based on the relative abundance of dominant bacteria at the genus level. The PCA analysis in the figure highlights distinct shifts in the microbial community composition

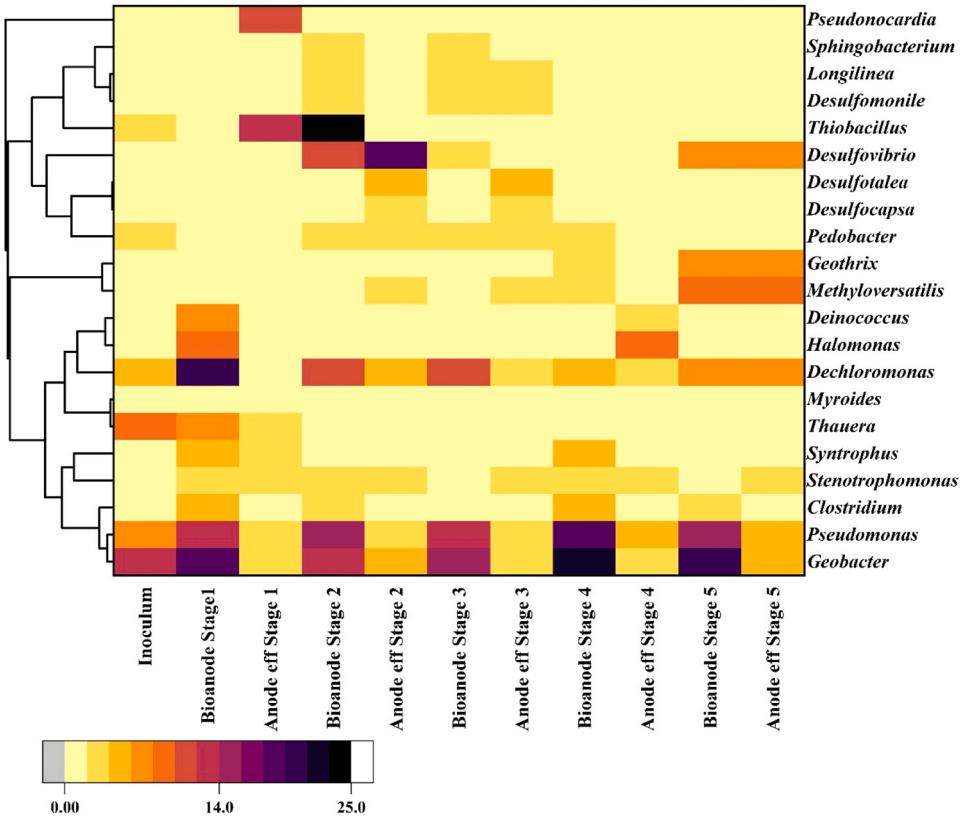

Fig. 5. Heat-map of relative abundance of dominant bacteria at the genus level in the microbial community from the anode chamber of the BEC reactor.

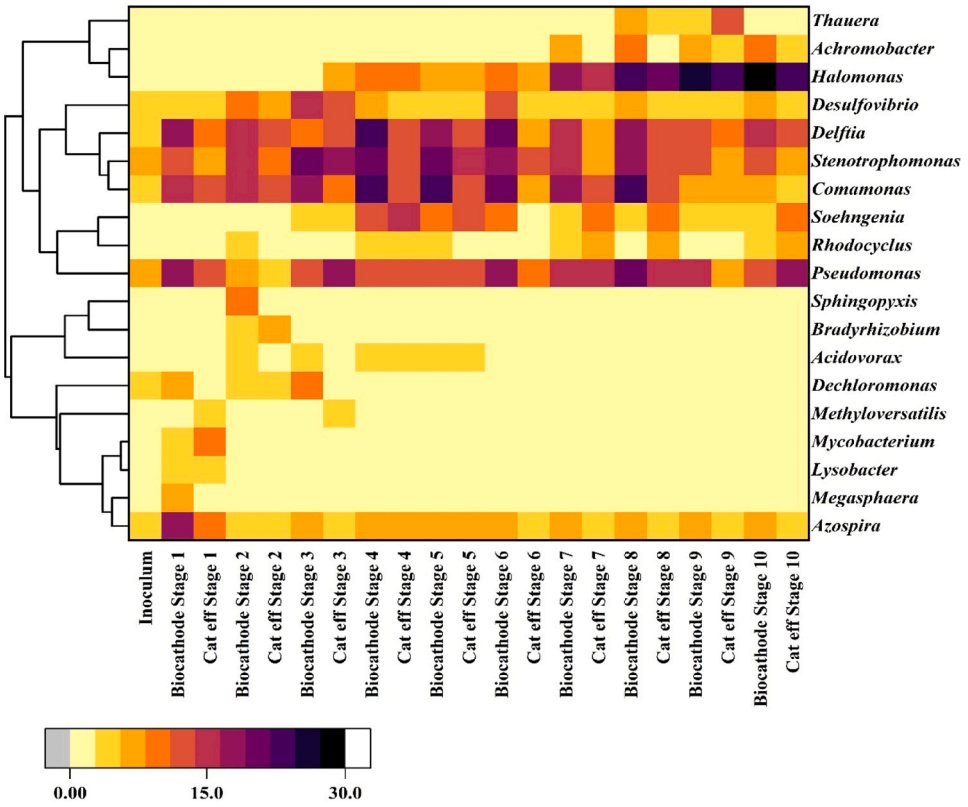

Fig. 6. Heat-map of relative abundance of dominant bacteria at the genus level in the microbial community from the cathode chamber of the BEC reactor.

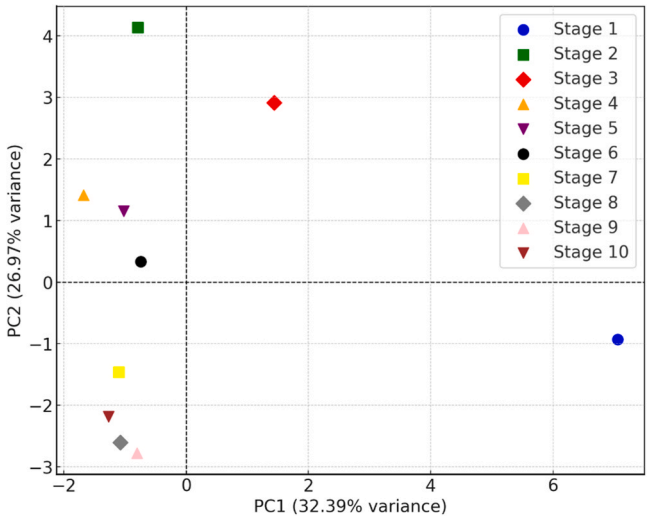

Fig. 7. Principal component analysis (PCA) showing the bacterial community grouping.

across different stages, which align with the variations in sulfate, selenate, and nitrate concentrations. PC1 and 2 revealed 32.39 % and 26.97 % of the entire community variations, respectively. The limited spread along PC1 indicates that the overall microbial community composition remained relatively stable. From stages 2–6, we observed a higher abundance of sulfate-reducing bacteria, consistent with the elevated sulfate levels, suggesting that these bacteria thrived under sulfate-rich conditions.

In stages 7–10, the gradual addition of nitrate (from 2.5 mg/L to 10 mg/L) coincided with a shift towards a higher relative abundance of denitrifying bacteria. This shift suggests that nitrate served as a significant electron acceptor, promoting the growth of bacteria capable of reducing nitrate. The PCA plot illustrates these shifts, with the stages clustering separately along the PC1 and PC2 axes, reflecting changes in microbial community composition driven by the varying electron acceptors (sulfate, nitrate, and selenate) across the different stages.

4. Conclusion

This research shows that the biocathode of the BEC reactor can effectively remove selenate at 5 mg Se/L in simulated wastewater, meeting the USEPA standard for selenium at 0.076 mg Se/L under certain operating conditions. The impact of high sulfate concentration (1000 mg S/L) on the BEC reactor was much lower than on the conventional biofilm reactor, with selenium removal reaching 99 % in the BEC reactor compared to 69 % in the conventional biofilm reactor. Particulate selenium can be potentially removed and recovered. The lower selenium removal in the conventional reactor was mainly due to the >10 times higher sulfate reduction, which competed with selenate for common resources such as electrons. This also led to greater selenide production: 0.9 mg Se/L in the conventional reactor versus 0.02 mg Se/L in the BEC reactor. Selenide is usually not measured in the literature and is assumed to be minimal. This simplification may significantly overestimate selenium removal. NO_3^- promoted selenium removal when $\leq$ 5.0 mg N/L, probably due to inducing selenate reductase. When NO_3^- concentration was 7.5 mg N/L or more, nitrate inhibited selenium removal due to competition for limited common resources such as electrons. This was supported by nitrite accumulation and microbial community analysis showing enrichment of denitrifying bacteria *Halomonas* at the high nitrate concentrations. The findings highlight the importance of optimizing retention time and microbial inoculum for better selenium reduction and recovery.

Given the increasing regulatory pressures to manage selenium contamination, this technology offers a viable solution for industries to meet stringent environmental standards and regulatory compliance. The potential for commercialization lies in its ability to provide an effective, cost-efficient, and environmentally sustainable method for removing selenium from wastewater.

Funding

This work was supported by the National Science Foundation (NSF) through grant number #2029682 awarded to Florida State University.

CRediT authorship contribution statement

Benhur K. Asefaw: Writing – original draft, Methodology, Investigation, Formal analysis, Conceptualization. **Huan Chen:** Writing – review & editing, Supervision, Resources, Methodology, Funding acquisition, Formal analysis. **Youneng Tang:** Writing – review & editing, Supervision, Resources, Methodology, Funding acquisition, Formal analysis, Conceptualization.

Declaration of Competing Interest

The authors declare that they have no known competing financial interests or personal relationships that could have appeared to influence the work reported in this paper.

Acknowledgements

The authors greatly thank Dr. Eric Lochner at Florida State University for providing technical support in the SEM. The SEM work was performed at the Condensed Matter and Material Physics facilities, Florida State University. The work conducted at the National High Magnetic Field Laboratory receives support from the NSF Division of Chemistry and Division of Materials Research through DMR-2128556, as well as the State of Florida.

Appendix A. Supporting information

Supplementary data associated with this article can be found in the online version at doi:10.1016/j.bej.2024.109531.

Data availability

Data will be made available on request.

References

[1] A.D. Lemly, Aquatic selenium pollution is a global environmental safety issue, Ecotoxicol. Environ. Saf. 59 (2004), https://doi.org/10.1016/S0147-6513(03)00095-2.
[2] F. Fordyce, Selenium geochemistry and health, Ambio (2007), https://doi.org/10.1579/0044-7447(2007)36[94:SGAH]2.0.CO;2.
[3] G.D. Jones, B. Droz, P. Greve, P. Gottschalk, D. Poffet, S.P. McGrath, S. I. Seneviratne, P. Smith, L.H.E. Winkel, Selenium deficiency risk predicted to increase under future climate change, Proc. Natl. Acad. Sci. U. S. A. 114 (2017), https://doi.org/10.1073/pnas.1611576114.
[4] Z. Zhang, Y. Xiong, H. Chen, Y. Tang, Understanding the composition and spatial distribution of biological selenate reduction products for potential selenium recovery, Environ. Sci. Water Res. Technol. (2020), https://doi.org/10.1039/d0ew00376j.
[5] R.S. Oremland, M.J. Herbel, J.S. Blum, S. Langley, T.J. Beveridge, P.M. Ajayan, T. Sutto, A.V. Ellis, S. Curran, Structural and spectral features of selenium nanospheres produced by Se-respiring bacteria, Appl. Environ. Microbiol. 70 (2004), https://doi.org/10.1128/AEM.70.1.52-60.2004.
[6] C.I. Pearce, R.A.D. Pattrick, N. Law, J.M. Charnock, V.S. Coker, J.W. Fellowes, R. S. Oremland, J.R. Lloyd, Investigating different mechanisms for biogenic selenite transformations: Geobacter sulfurreducens, Shewanella oneidensis and Veillonella atypica, Environ. Technol. 30 (2009), https://doi.org/10.1080/09593330902984751.
[7] G. Sharma, A.R. Sharma, R. Bhavesh, J. Park, B. Ganbold, J.S. Nam, S.S. Lee, Biomolecule-mediated synthesis of selenium nanoparticles using dried Vitis

vinifera (raisin) extract, Molecules 19 (2014), https://doi.org/10.3390/molecules19032761.
[8] USEPA, Drinking Water Contaminants: National Primary Drinking Water Regulations, US EPA Website ⟨Http//Water.Epa.Gov/Drink/Contaminants/Index.Cfm⟩ (2015).
[9] USEPA, Title 40-Chapter 1-CFR Part 423, Effluent Limitations Guidelines and Standards for the Steam Electric Power Generating Point Source Category, Fed. Regist. Vol. 85, No. 198 (2019). ⟨https://www.federalregister.gov/documents/2019/11/22/2019-24686/effluent-limitations-guidelines-and-standards-for-the-steam-electric-power-generating-point-source⟩ (accessed January 12, 2023).
[10] C. Bernhardt, A. Russ, E. Schaeffer, Toxic Wastewater from Coal Plants, 2016. ⟨https://www.environmentalintegrity.org/wp-content/uploads/2016/11/Toxic-Wastewater-from-Coal-Plants-2016.08.11-1.pdf⟩.
[11] P.M. Haygarth, Global importance and global cycling of selenium, Selenium Environ. (1994).
[12] J.G. Price, Energy critical elements: securing materials for emerging technologies, Min. Eng. 63 (2011).
[13] U.S. Geological Survey, Historical statistics for mineral and material commodities in the United States (2015 version): U.S. Geological Survey Data Series 140, Miner. Commod. Gold (2015).
[14] M. Twidwell, L.G., McCloskey, J.M., Miranda, P., Gale, Technologies and potential technologies for removing selenium from process and mine wastewater. In: Gaballah, I., Hager, J., Solozaral, R. (Eds.), Glob Symp Recycl Waste Treat CleanTechnol.San Sabastian, Spain (1999) 1645–1656.
[15] S. Santos, G. Ungureanu, R. Boaventura, C. Botelho, Selenium contaminated waters: an overview of analytical methods, treatment options and recent advances in sorption methods, Sci. Total Environ. 521–522 (2015) 246–260, https://doi.org/10.1016/J.SCITOTENV.2015.03.107.
[16] Z. Ma, C. Shan, J. Liang, M. Tong, Efficient adsorption of Selenium(IV) from water by hematite modified magnetic nanoparticles, Chemosphere (2018), https://doi.org/10.1016/j.chemosphere.2017.11.005.
[17] K. Kalaitzidou, A.A. Nikoletopoulos, N. Tsiftsakis, F. Pinakidou, M. Mitrakas, Adsorption of Se(IV) and Se(VI) species by iron oxy-hydroxides: effect of positive surface charge density, Sci. Total Environ. (2019), https://doi.org/10.1016/j.scitotenv.2019.06.174.
[18] T. Nakajima, K. Yamada, H. Idehara, H. Takanashi, A. Ohki, Removal of selenium (VI) from simulated wet flue gas desulfurization wastewater using photocatalytic reduction, J. Water Environ. Technol. (2011), https://doi.org/10.2965/jwet.2011.13.
[19] A.B. Holmes, D. Khan, D. De Oliveira Livera, F. Gu, Enhanced photocatalytic selectivity of noble metallized TiO2nanoparticles for the reduction of selenate in water: tunable Se reduction product H2Se(g): vs. Se(s), Environ. Sci. Nano (2020), https://doi.org/10.1039/d0en00048e.
[20] Y.K. Kharaka, G. Ambats, T.S. Presser, R.A. Davis, Removal of selenium from contaminated agricultural drainage water by nanofiltration membranes, Appl. Geochem. 11 (1996), https://doi.org/10.1016/S0883-2927(96)00044-3.
[21] T. Sandy, C. DiSante, Review of available technologies for the removal of selenium from water, North Am. Met. Counc. (2010).
[22] S. Soda, M. Kashiwa, T. Kagami, M. Kuroda, M. Yamashita, M. Ike, Laboratory-scale bioreactors for soluble selenium removal from selenium refinery wastewater using anaerobic sludge, Desalination 279 (2011), https://doi.org/10.1016/j.desal.2011.06.031.
[23] Y. Zhang, W.T. Frankenberger, Removal of selenate in river and drainage waters by Citrobacter braakii enhanced with zero-valent iron, J. Agric. Food Chem. (2006), https://doi.org/10.1021/jf058124o.
[24] C. Tang, Y.H. Huang, H. Zeng, Z. Zhang, Reductive removal of selenate by zero-valent iron: the roles of aqueous Fe2+ and corrosion products, and selenate removal mechanisms, Water Res (2014), https://doi.org/10.1016/j.watres.2014.09.016.
[25] T. Nishimura, H. Hashimoto, M. Nakayama, Removal of selenium(VI) from aqueous solution with polyamine-type weakly basic ion exchange resin, Sep. Sci. Technol. (2007), https://doi.org/10.1080/01496390701513107.
[26] Y.T. Chan, Y.T. Liu, Y.M. Tzou, W.H. Kuan, R.R. Chang, M.K. Wang, Kinetics and equilibrium adsorption study of selenium oxyanions onto Al/Si and Fe/Si coprecipitates, Chemosphere (2018), https://doi.org/10.1016/j.chemosphere.2018.01.110.
[27] C.Y. Lai, L.L. Wen, L.D. Shi, K.K. Zhao, Y.Q. Wang, X. Yang, B.E. Rittmann, C. Zhou, Y. Tang, P. Zheng, H.P. Zhao, Selenate and nitrate bioreductions using methane as the electron donor in a membrane biofilm reactor, Environ. Sci. Technol. (2016), https://doi.org/10.1021/acs.est.6b02807.
[28] W. Han, Y. Mao, Y. Wei, P. Shang, X. Zhou, Bioremediation of aquaculture wastewater with algal-bacterial biofilm combined with the production of selenium rich biofertilizer, Water (2020), https://doi.org/10.3390/w12072071.
[29] Z. Zhang, B.K. Asefaw, Y. Xiong, H. Chen, Y. Tang, Evidence and mechanisms of selenate reduction to extracellular elemental selenium nanoparticles on the biocathode, Environ. Sci. Technol. 56 (2022) 16259–16270, https://doi.org/10.1021/acs.est.2c05145.
[30] S. Yan, K.Y. Cheng, T. Bohu, C. Morris, L. Lomheim, I. Yang, M.P. Ginige, E. Edwards, G. Zheng, L. Zhou, A.H. Kaksonen, Microbial community dynamics in a feedback-redox controlled bioreactor process that enabled sequential selenate, nitrate and sulfate removal, and elemental selenium recovery, J. Water Process Eng. (2023), https://doi.org/10.1016/j.jwpe.2023.103881.
[31] Z. Zhang, G. Chen, Y. Tang, Towards selenium recovery: biocathode induced selenate reduction to extracellular elemental selenium nanoparticles, Chem. Eng. J. 351 (2018), https://doi.org/10.1016/j.cej.2018.06.172.
[32] L.C. Tan, E.J. Espinosa-Ortiz, Y.V. Nancharaiah, E.D. van Hullebusch, R. Gerlach, P.N.L. Lens, Selenate removal in biofilm systems: effect of nitrate and sulfate on selenium removal efficiency, biofilm structure and microbial community, J. Chem. Technol. Biotechnol. (2018), https://doi.org/10.1002/jctb.5586.
[33] S. Yan, K.Y. Cheng, M.P. Ginige, C. Morris, X. Deng, J. Li, S. Song, G. Zheng, L. Zhou, A.H. Kaksonen, Sequential removal of selenate, nitrate and sulfate and recovery of elemental selenium in a multi-stage bioreactor process with redox potential feedback control, J. Hazard. Mater. (2022), https://doi.org/10.1016/j.jhazmat.2021.127539.
[34] M. Lenz, P.N.L. Lens, The essential toxin: the changing perception of selenium in environmental sciences, Sci. Total Environ. 407 (2009), https://doi.org/10.1016/j.scitotenv.2008.07.056.
[35] N.W.T. Quinn, T. Leighton, T.J. Lundquist, F.B. Green, M.A. Zárate, W.J. Oswald, Algal-bacterial treatment facility removes selenium from drainage water, Calif. Agric. (2000), https://doi.org/10.3733/ca.v054n06p50.
[36] Z. Zhang, Y. Tang, Comparing methods for measuring dissolved and particulate selenium in water, J. Water Environ. Technol. 18 (2020), https://doi.org/10.2965/jwet.20-003.
[37] J.P. Zehr, R.S. Oremland, Reduction of selenate to selenide by sulfate-respiring bacteria: experiments with cell suspensions and estuarine sediments, Appl. Environ. Microbiol. 53 (1987), https://doi.org/10.1128/aem.53.6.1365-1369.1987.
[38] S. Hockin, G.M. Gadd, Removal of selenate from sulfate-containing media by sulfate-reducing bacterial biofilms, Environ. Microbiol. 8 (2006), https://doi.org/10.1111/j.1462-2920.2005.00967.x.
[39] L.C. Tan, Y.V. Nancharaiah, E.D. van Hullebusch, P.N.L. Lens, Selenium: environmental significance, pollution, and biological treatment technologies, Anaerob. Treat. Mine Wastewater Remov. Selenate Its Co. -Contam. (2018), https://doi.org/10.1201/9780429448676-2.
[40] J.P. Zehr, R.S. Oremland, Reduction of selenate to selenide by sulfate-respiring bacteria: experiments with cell suspensions and estuarine sediments, Appl. Environ. Microbiol. (1987), https://doi.org/10.1128/aem.53.6.1365-1369.1987.
[41] N. Geoffroy, G.P. Demopoulos, The elimination of selenium(IV) from aqueous solution by precipitation with sodium sulfide, J. Hazard. Mater. 185 (2011), https://doi.org/10.1016/j.jhazmat.2010.09.009.
[42] Y.V. Nancharaiah, S. Venkata Mohan, P.N.L. Lens, Metals removal and recovery in bioelectrochemical systems: a review, Bioresour. Technol. 195 (2015), https://doi.org/10.1016/j.biortech.2015.06.058.
[43] T. Zhang, H. Yu, Y. Dai, Z. Wang, D. Yang, F. Qiu, Coupling adsorption and reduction for tellurium recovery by hierarchical porous nanoscale zero-valent iron (NZVI) /LDOs composites, Results Eng. (2022), https://doi.org/10.1016/j.rineng.2022.100356.
[44] L.B. Jugnia, D. Manno, A.G. Vidales, S. Hrapovic, B. Tartakovsky, Selenite and selenate removal in a permeable flow-through bioelectrochemical barrier, J. Hazard. Mater. (2021), https://doi.org/10.1016/j.jhazmat.2020.124431.
[45] C.Y. Lai, X. Yang, Y. Tang, B.E. Rittmann, H.P. Zhao, Nitrate shaped the selenate-reducing microbial community in a hydrogen-based biofilm reactor, Environ. Sci. Technol. 48 (2014), https://doi.org/10.1021/es4053939.
[46] J.F. Stolz, R.S. Oremland, Bacterial respiration of arsenic and selenium, FEMS Microbiol. Rev. 23 (1999), https://doi.org/10.1016/S0168-6445(99)00024-8.
[47] N.A. Steinberg, J.S. Blum, L. Hochstein, R.S. Oremland, Nitrate is a preferred electron acceptor for growth of freshwater selenate-respiring bacteria, Appl. Environ. Microbiol. 58 (1992), https://doi.org/10.1128/aem.58.1.426-428.1992.
[48] J.M. Macy, S. Lawson, H. DeMoll-Decker, Bioremediation of selenium oxyanions in San Joaquin drainage water using Thauera selenatis in a biological reactor system, Appl. Microbiol. Biotechnol. 40 (1993), https://doi.org/10.1007/BF00175752.
[49] C. Garbisu, T. Ishii, T. Leighton, B.B. Buchanan, Bacterial reduction of selenite to elemental selenium, Chem. Geol. 132 (1996), https://doi.org/10.1016/s0009-2541(96)00056-3.
[50] R.S. Dungan, S.R. Yates, W.T. Frankenberger, Transformations of selenate and selenite by Stenotrophomonas maltophilia isolated from a seleniferous agricultural drainage pond sediment, Environ. Microbiol. 5 (2003), https://doi.org/10.1046/j.1462-2920.2003.00410.x.
[51] H. DeMoll-Decker, J.M. Macy, The periplasmic nitrite reductase of Thauera selenatis may catalyze the reduction of selenite to elemental selenium, Arch. Microbiol. 160 (1993), https://doi.org/10.1007/BF00249131.
[52] M. Sabaty, C. Avazeri, D. Pignol, A. Vermeglio, Characterization of the reduction of selenate and tellurite by nitrate reductases, Appl. Environ. Microbiol. (2001), https://doi.org/10.1128/aem.67.11.5122-5126.2001.
[53] B. Environmental Laboratory Manual, Sulfide in Water by Colourimetric Analysis - PBM, n.d. ⟨https://www2.gov.bc.ca/assets/gov/environment/research-monitoring-and-reporting/monitoring/emre/methods/sulfide_in_water_by_colourimetric_analysis_-_pbm.pdf⟩.
[54] S. Tanaka, K. Sugawara, M. Taga, Voltammetry of Selenium(IV) Based on an Adsorptive Accumulation of Selenium-2,3-Diaminonaphthalene Complex, Anal. Sci. (1990), https://doi.org/10.2116/analsci.6.475.
[55] P. Cukor, P.F. Lott, The kinetics of the reaction of selenium(IV) with 2,3-diaminonaphthalene, J. Phys. Chem. (1965), https://doi.org/10.1021/j100894a002.
[56] V.S. Pylro, L.F.W. Roesch, D.K. Morais, I.M. Clark, P.R. Hirsch, M.R. Tótola, Data analysis for 16S microbial profiling from different benchtop sequencing platforms, J. Microbiol. Methods 107 (2014), https://doi.org/10.1016/j.mimet.2014.08.018.
[57] D. Ionescu, W.A. Overholt, M.D.J. Lynch, J.D. Neufeld, A. Naqib, S.J. Green, Microbial community analysis using high-throughput amplicon sequencing, Man. Environ. Microbiol. (2015), https://doi.org/10.1128/9781555818821.ch2.4.2.

[58] R.L. Barter, B. Yu, Superheat: an R package for creating beautiful and extendable heatmaps for visualizing complex data, J. Comput. Graph. Stat. 27 (2018), https://doi.org/10.1080/10618600.2018.1473780.
[59] D. Wang, C. Rensing, S. Zheng, Microbial reduction and resistance to selenium: mechanisms, applications and prospects, J. Hazard. Mater. (2022), https://doi.org/10.1016/j.jhazmat.2021.126684.
[60] Y. Tang, C.J. Werth, R.A. Sanford, R. Singh, K. Michelson, M. Nobu, W.T. Liu, A. J. Valocchi, Immobilization of selenite via two parallel pathways during in situ bioremediation, Environ. Sci. Technol. (2015), https://doi.org/10.1021/es506107r.
[61] H.K. Shrimpton, C.J. Ptacek, D.W. Blowes, Selenite stable isotope fractionation during abiotic reduction by sodium sulfide, Environ. Sci. Technol. (2024), https://doi.org/10.1021/acs.est.4c03607.
[62] D.R. Bond, D.R. Lovley, Electricity production by Geobacter sulfurreducens attached to electrodes, Appl. Environ. Microbiol. 69 (2003), https://doi.org/10.1128/AEM.69.3.1548-1555.2003.
[63] C.C. Chang, Y.C. Chen, C.P. Yu, Microbial community dynamics in electroactive biofilms across time under different applied anode potentials, Sustain. Environ. Res. 32 (2022), https://doi.org/10.1186/s42834-022-00128-9.
[64] F. Allam, M. Elnouby, S.A. Sabry, K.M. El-Khatib, D.E. El-Badan, Optimization of factors affecting current generation, biofilm formation and rhamnolipid production by electroactive Pseudomonas aeruginosa FA17, Int. J. Hydrog. Energy 46 (2021), https://doi.org/10.1016/j.ijhydene.2020.08.070.
[65] A. Kaushik, S.K. Jadhav, Conversion of waste to electricity in a microbial fuel cell using newly identified bacteria: Pseudomonas fluorescens, Int. J. Environ. Sci. Technol. (2017), https://doi.org/10.1007/s13762-017-1260-z.
[66] B.J. Eddie, S.M. Glaven, Electrified biofilms: a special issue on microbial electrochemistry, Biofilm 3 (2021), https://doi.org/10.1016/j.bioflm.2021.100062.
[67] L. Zhang, G. Fu, Z. Zhang, Electricity generation and microbial community in long-running microbial fuel cell for high-salinity mustard tuber wastewater treatment, Bioelectrochemistry 126 (2019), https://doi.org/10.1016/j.bioelechem.2018.11.002.
[68] I. Ulusoy, A. Dimoglo, Electricity generation in microbial fuel cell systems with Thiobacillus ferrooxidans as the cathode microorganism, Int. J. Hydrog. Energy (2018), https://doi.org/10.1016/j.ijhydene.2017.10.155.
[69] G. Ranalli, E. Zanardini, C. Sorlini, Biodeterioration - including cultural heritage, : Encycl. Microbiol. (2019), https://doi.org/10.1016/B978-0-12-809633-8.13016-X.
[70] A. Ghosh, A.M. Mohod, K.M. Paknikar, R.K. Jain, Isolation and characterization of selenite- and selenate-tolerant microorganisms from selenium-contaminated sites, World J. Microbiol. Biotechnol. (2008), https://doi.org/10.1007/s11274-007-9624-z.
[71] S. Zheng, J. Su, L. Wang, R. Yao, D. Wang, Y. Deng, R. Wang, G. Wang, C. Rensing, Selenite reduction by the obligate aerobic bacterium, BMC Microbiol (2014).
[72] G. Gonzalez-Gil, P.N.L. Lens, P.E. Saikaly, Selenite reduction by anaerobic microbial aggregates: microbial community structure, and proteins associated to the produced selenium spheres, Front. Microbiol. (2016), https://doi.org/10.3389/fmicb.2016.00571.
[73] K. Venkidusamy, M. Megharaj, Identification of electrode respiring, hydrocarbonoclastic bacterial strain Stenotrophomonas maltophilia MK2 highlights the untapped potential for environmental bioremediation, Front. Microbiol. 7 (2016), https://doi.org/10.3389/fmicb.2016.01965.
[74] K. Becerril-Varela, J.H. Serment-Guerrero, G.L. Manzanares-Leal, N. Ramírez-Durán, C. Guerrero-Barajas, Generation of electrical energy in a microbial fuel cell coupling acetate oxidation to Fe3+ reduction and isolation of the involved bacteria, World J. Microbiol. Biotechnol. 37 (2021), https://doi.org/10.1007/s11274-021-03077-4.
[75] F.A. Tomei, L.L. Barton, C.L. Lemanski, T.G. Zocco, N.H. Fink, L.O. Sillerud, Transformation of selenate and selenite to elemental selenium by Desulfovibrio desulfuricans, J. Ind. Microbiol. 14 (1995), https://doi.org/10.1007/BF01569947.
[76] Y. Xie, X. Tian, Y. He, S. Dong, K. zhao, Nitrogen removal capability and mechanism of a novel heterotrophic nitrification–aerobic denitrification bacterium Halomonas sp. DN3, Bioresour. Technol. (2023), https://doi.org/10.1016/j.biortech.2023.129569.
[77] T. Wang, Z. Jiang, W. Dong, X. Liang, L. Zhang, Y. Zhu, Growth and nitrogen removal characteristics of Halomonas sp. B01 under high salinity, Ann. Microbiol. (2019), https://doi.org/10.1007/s13213-019-01526-y.
[78] A. Ontiveros-Valencia, C.R. Penton, R. Krajmalnik-Brown, B.E. Rittmann, Hydrogen-fed biofilm reactors reducing selenate and sulfate: community structure and capture of elemental selenium within the biofilm, Biotechnol. Bioeng. 113 (2016), https://doi.org/10.1002/bit.25945.
[79] L. Zhou, X. Xu, S. Xia, Effects of sulfate on simultaneous nitrate and selenate removal in a hydrogen-based membrane biofilm reactor for groundwater treatment: Performance and biofilm microbial ecology, Chemosphere (2018), https://doi.org/10.1016/j.chemosphere.2018.07.092.
[80] J. Chung, R. Nerenberg, B.E. Rittmann, Bioreduction of selenate using a hydrogen-based membrane biofilm reactor, Environ. Sci. Technol. (2006), https://doi.org/10.1021/es051251g.
[81] L.C. Tan, S. Papirio, V. Luongo, Y.V. Nancharaiah, P. Cennamo, G. Esposito, E. D. van Hullebusch, P.N.L. Lens, Comparative performance of anaerobic attached biofilm and granular sludge reactors for the treatment of model mine drainage wastewater containing selenate, sulfate and nickel, Chem. Eng. J. (2018), https://doi.org/10.1016/j.cej.2018.03.177.
[82] J.M. Macy, S. Lawson, H. DeMoll-Decker, Bioremediation of selenium oxyanions in San Joaquin drainage water using Thauera selenatis in a biological reactor system, Appl. Microbiol. Biotechnol. (1993), https://doi.org/10.1007/BF00175752.
[83] S. Yan, K.Y. Cheng, M.P. Ginige, G. Zheng, L. Zhou, A.H. Kaksonen, Optimization of nitrate and selenate reduction in an ethanol-fed fluidized bed reactor via redox potential feedback control, J. Hazard. Mater. (2021), https://doi.org/10.1016/j.jhazmat.2020.123770.
[84] H. Sonkeshariya, A.K. Shakya, P.K. Ghosh, Development of a sulfidogenic bioreactor system for removal of co-existent selenium, iron and nitrate from drinking water sources, J. Environ. Manag. (2020), https://doi.org/10.1016/j.jenvman.2019.109757.
[85] L.C. Tan, Y.V. Nancharaiah, S. Lu, E.D. van Hullebusch, R. Gerlach, P.N.L. Lens, Biological treatment of selenium-laden wastewater containing nitrate and sulfate in an upflow anaerobic sludge bed reactor at pH 5.0, Chemosphere (2018), https://doi.org/10.1016/j.chemosphere.2018.07.079.
[86] L.C. Tan, Y.V. Nancharaiah, E.D. Van Hullebusch, P.N.L. Lens, Effect of elevated nitrate and sulfate concentrations on selenate removal by mesophilic anaerobic granular sludge bed reactors, Environ. Sci. Water Res. Technol. (2018), https://doi.org/10.1039/c7ew00307b.
[87] M. Lenz, A.M. Enright, V. O'Flaherty, A.C. Van Aelst, P.N.L. Lens, Bioaugmentation of UASB reactors with immobilized Sulfurospirillum barnesii for simultaneous selenate and nitrate removal, Appl. Microbiol. Biotechnol. (2009), https://doi.org/10.1007/s00253-009-1915-x.
[88] M. Lenz, E.D.V. Hullebusch, G. Hommes, P.F.X. Corvini, P.N.L. Lens, Selenate removal in methanogenic and sulfate-reducing upflow anaerobic sludge bed reactors, Water Res (2008), https://doi.org/10.1016/j.watres.2007.11.031.